Up to 10.7-Gb/s High-PDG RSOA-Based Colorless Transmitter for WDM Networks

Lucia Marazzi, Paola Parolari, Marco Brunero, Alberto Gatto, Mario Martinelli, Romain Brenot, Sophie Barbet, Paola Galli, and Giancarlo Gavioli

***Abstract*— The operation of a network-embedded colorless self-tuning transmitter for WDM networks is experimentally demonstrated from 2.5- up to 10.7-Gb/s data rates. Colorless operation is achieved by self-seeding an ultra-fast reflective semiconductor optical amplifier (RSOA) with the feedback signal reflected at the WDM multiplexer filter. In particular, the transmitter exploits a 2-Faraday rotators configuration to ensure polarization insensitive operation and allowing for the exploitation of high gain RSOAs, which can be designed to operate on a single polarization. The impact on the transmission of the fiber chromatic dispersion at different bit-rates and with different channel bandwidths of the WDM multiplexer filter is experimentally investigated up to 10.7 Gb/s. The tolerance to positive and negative dispersive loads is also assessed.**

***Index Terms*— Passive optical network (PON), polarization, reflective semiconductor optical amplifier (RSOA), retracing optical circuit.**

I. Introduction

A COLOR-AGNOSTIC optical network unit (ONU) is a recognized requirement for next generation access networks (NGAN). Color-free or colorless solutions have been obtained for instance with tunable lasers, which offer high-speed and long-reach transmission [1], nevertheless requiring a wavelength detection algorithm to automatically set and maintain the proper allocated wavelength [2]. ONUs exploiting injection in Fabry-Perot [3] and reflective semiconductor optical amplifier-based (RSOA) [4] can be forced to operate at the proper allocated wavelength and thus be colorless, at the expense of external seeding sources. A smart solution avoiding the need of these external sources, and consequently also Rayleigh scattering impairments, as well as wavelength detection algorithms, is represented by the self-seeded RSOA, which implements a self-tuning transmitter. A major issue with RSOA self-seeded architecture is the polarization evolution within the optical circuit [5], which is established between the optical reflector at the remote node (RN) and the mirror at the reflective semiconductor optical amplifier, placed at the ONU. The distribution fiber, which connects the ONU and the RN WDM multiplexer, namely an arrayed waveguide grating (AWG), can range from a hundred of meters to a few kilometers. The unavoidable birefringence of the fiber modifies in an unpredictable manner the state of polarization (SOP) of the signal returning to the RSOA after the remote mirror reflection and the transit into the AWG.

The problem has been solved for low-polarization dependent gain (PDG) RSOA [6], [7] exploiting the properties of the Faraday rotator mirror, known as the universal time-reversal operator, which ensures that the SOP of the signal re-injected in the RSOA is orthogonally aligned to the signal at the RSOA output. 1.25-Gb/s operation of a 32-channels WDM PON exploiting self-seeded transmitters has been demonstrated for low-PDG RSOA [7]. Yet the possibility to disregard the PDG issue in RSOA project allows designing the active section, aiming at either larger saturation power, smaller noise factor, or better temperature stability of the gain, for example by using compressively strained multi-quantum wells or quantum dots [8], thus pursuing faster and more efficient devices, with high PDG. Recently a theoretical analysis and CW experimental measurements [9] have demonstrated that a two-Faraday topology allows exploitation of high-PDG RSOAs in self-tuning transmitters. A similar self-seeding configuration has been demonstrated with Fabry-Perot lasers at 1.25 Gb/s achieving performances close to low-PDG RSOA-based configurations [10].

In this letter we focus on the case of high-PDG RSOAs analyzing the impact on the transmission of the fiber chromatic dispersion at different bit-rates, from 2.5 Gb/s up to 10.7 Gb/s, and for different AWG full width half maximum (FWHM) channel bandwidth. Finally we demonstrate for the first time, to the best of our knowledge, the operation of the two-Faraday rotator-based optical circuit at 10.7 Gb/s bridging more that 50 km of negative non-zero dispersion shifted (NZD^-) optical fiber.

II. Polarization Insensitive Retracing Optical Circuit Experimental Setup

The optical circuit, which implements the polarization insensitive transmitter, is described in the experimental setup shown in Fig. 1. As described in [7], the RSOA plays the triple role of sustaining the cavity gain, of modulating the

Manuscript received November 9, 2012; revised January 10, 2013; accepted January 15, 2013. Date of publication January 28, 2013; date of current version March 12, 2013. This work was supported in part by the European Union's Seventh Framework Programme under Grant FP7/2007-2013, and in part by Grant Agreement ERMES n° 288542 2012.

L. Marazzi, P. Parolari, M. Brunero, A. Gatto, and M. Martinelli are with the Department Electronics and Information - PoliCom, Politecnico di Milano, Milan 20133, Italy (e-mail: marazzi@elet.polimi.it; pparolari@elet.polimi.it; brunero@elet.polimi.it; agatto@elet.polimi.it; martinelli@elet.polimi.it).

R. Brenot and S. Barbet are with the III–V Laboratory, Alcatel-Lucent Bell Labs France, Marcoussis 91460, France (e-mail: brenot@3-5lab.fr; sophie.barbet@3-5lab.fr).

P. Galli and G. Gavioli are with Alcatel-Lucent Italia, Vimercate 20871, Italy (e-mail: paola.galli@alcatel-lucent.com; giancarlo.gavioli@alcatel-lucent.com).

Color versions of one or more of the figures in this letter are available online at http://ieeexplore.ieee.org.

Digital Object Identifier 10.1109/LPT.2013.2243138

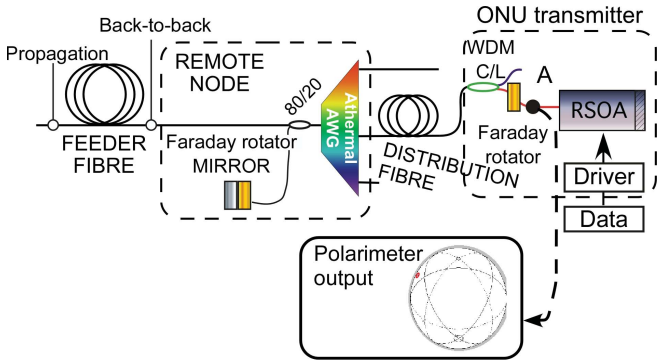

Fig. 1. Experimental setup of the polarization insensitive retracing circuit. Inset: experimentally measured signal SOP on the Poincaré sphere.

transmitted signal via its bias current and of bleaching the recirculating modulation inside the cavity.

To allow the exploitation of high PDG RSOAs the addition of two simple elements is crucial: a Faraday rotator (FR), located in close proximity to the RSOA output, and a Faraday mirror, shared by all the ONUs and placed at the RN close to the AWG.

Thanks to the properties of this retracing circuit, which can be described by resorting to the Poincaré sphere [9], the polarization at the RSOA input is stable and aligned with the RSOA high gain transverse mode, showing a high degree of polarization. The joint effect of the FR at the ONU and of the Faraday rotator mirror (FRM) at the remote node ensures that the actions of the optical couplers, fibers and AWG, which can all be regarded as retarder wave plates, are retraced back so that the returning SOP is aligned with the initial signal SOP, which is aligned to the RSOA high gain transverse mode.

III. BER Evaluation

The colorless transmitter, whose experimental setup is shown in Fig. 1, exploits a purposely designed compressively strained multi quantum well (MQW) RSOA, which has more than 20-dB PDG and a measured E/O bandwidth of approximately 4 GHz. At 100 mA bias current, the RSOA presents the gain peak at 1530 nm, the measured small signal gain is 30 dB and 6-dB ER compression can be achieved at -7 dBm input power. The colorless transmitter is tested at different bit rates, from 2.5 to 10.7 Gb/s (OTN G.709), and for different AWG bandwidths, from 55 GHz to 220 GHz FWHM. The AWG transfer function is obtained using a tunable filter, which mimics a Gaussian athermal AWG profile. The 900-m long cavity has nearly 16-dB losses, which are due to the insertion losses of the FR (0.7 dB), the C/L WDM coupler (0.58 dB), the distribution fiber with various splicer and connectors (1.35 dB), the filter (3.95 dB) and the 80/20-output coupler (1.1 dB), which are passed twice, plus the FRM insertion losses of 0.5 dB.

Experimental results for 2.5 Gb/s are presented in Fig. 2, obtained using a 2.5 GHz-bandwidth APD receiver with clock and data recovery. The bias current is 108 mA and the ER obtained with 2.6 V peak-to-peak data voltage is 5.8 dB. Negligible penalties are present in back-to-back between transmitter exploiting the 220-GHz and 110-GHz AWG, these penalties become more significant at BER lower than 10^{-8}, while the transmitter with the 55-GHz AWG shows an

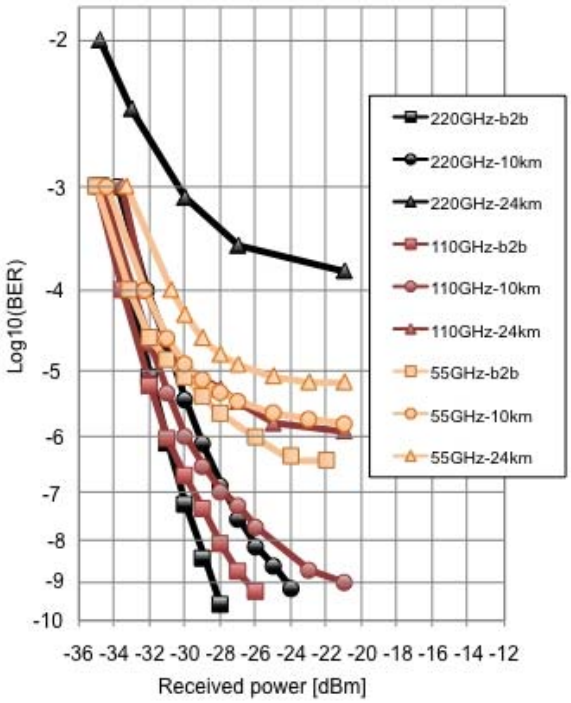

Fig. 2. BER measurements at 2.5 Gb/s for 220-GHz FWHM AWG (black), 110-GHz FWHM AWG (red), and 55-GHz FWHM AWG (orange). Propagation lengths of 10 (circles) and 24 km (triangles) of SSMF are considered and compared with back-to-back (squares).

increased error floor. The floor rises from under 10^{-10} to $5{\cdot}10^{-7}$ due to the tighter AWG spectral filtering, which results in increased relative intensity noise (RIN) on the transmitter output signal and thus reduces system performance [11]. After 10-km transmission over standard single mode fiber (SSMF), a marginal difference is found between the performances achieved with 220-GHz and 110-GHz AWG FWHM, while with tighter AWG filtering an evident error floor is present. After 24-km SSMF transmission, both the transmitter with 110-GHz AWG and with 55-GHz AWG outperform the 220-GHz AWG. The transmitter exploiting the widest filtering exhibits the worst transmission performance, as it corresponds to the widest modulated output optical spectrum. This can be seen for instance in Fig. 3, where the AWG normalized transfer functions are plotted together with the corresponding output modulated spectra. It can be thus concluded that, after 24-km SSMF, the accumulated chromatic dispersion becomes the limiting factor for the system performance. The best trade-off between chromatic dispersion penalties and RIN penalties is obtained for the 110-GHz AWG (red triangles in Fig. 2).

The 5 Gb/s BER curves are displayed in Fig. 3, the receiver is a 10-GHz APD followed by a 3-GHz Bessel electrical filter, chosen to limit the wide-bandwidth receiver noise. It is noteworthy that the RSOA E/O bandwidth is 4 GHz. The employed bias current is 102 mA and the ER obtained with 2.8 V peak-to-peak data voltage is 5.6 dB. The same AWG shapes and bandwidths as for the 2.5-Gb/s experiments are here employed, while propagation is limited to 10 km of SSMF without any electronic digital equalization. Similarly to the 2.5 Gb/s results, a marginal penalty difference is found in back to back for BER up to 10^{-6} between the performances

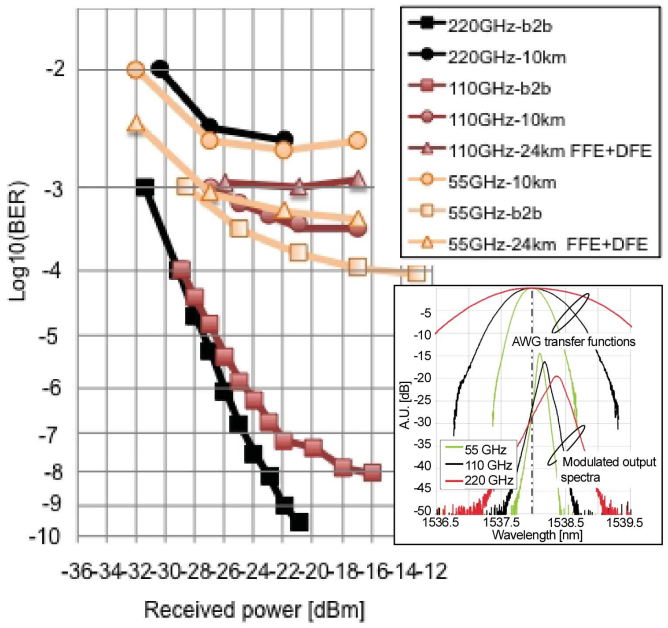

Fig. 3. BER measurements at 5 Gb/s for 220-GHz FWHM AWG (black), 110-GHz FWHM AWG (red), 55-GHz FWHM AWG (orange). Propagation lengths of 10 km (circles) of SSMF are considered and compared with back-to-back (squares). Inset: experimentally-exploited AWGs transfer functions with 220-GHz FWHM (red), 110 GHz FWHM (black) and 55-GHz FWHM (green) compared with the corresponding back-to-back 5-Gb/s modulated optical spectra.

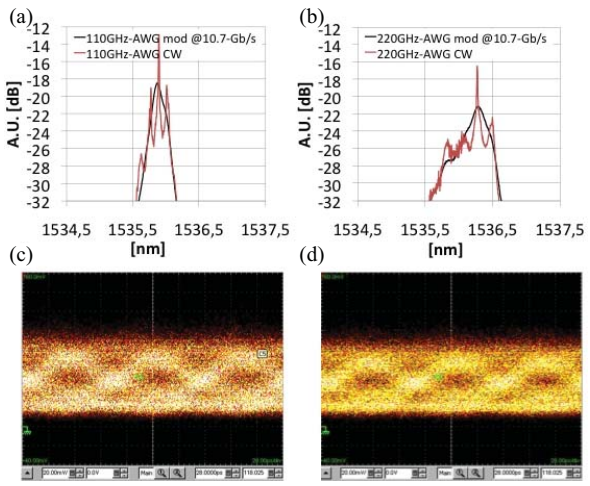

Fig. 4. CW and 10.7-Gb/s modulated spectra (a) 110-GHz FWHM AWG and (b) 220-GHz FWHM AWG. Back-to-back eye diagrams: (c) 110-GHz FWHM AWG and (d) 220-GHz FWHM AWG.

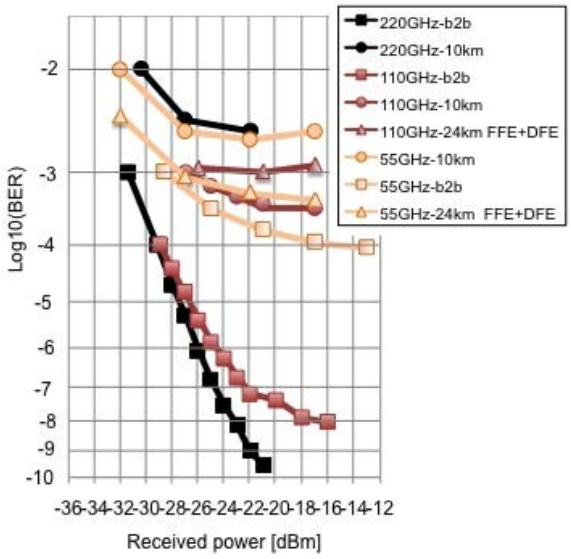

Fig. 5. OC192 (circles) and 10.7-Gb/s (triangles) BER curves in back-to-back (open symbols) and after 20 km of DS fiber (full symbols). Black and orange curves refer, respectively, to the transmitter with 220-GHz FWHM AWG and with 110-GHz FWHM AWG. The grey dotted-line curve refers to externally modulated laser. A commercially available digital equalizer with nine-taps FFE and four-taps DFE is employed.

achieved with the two largest AWG FWHMs, the 110-GHz AWG presenting an error floor at 10^{-8}. With 55-GHz filtering the error floor rises to 10^{-4}. As previously discussed, after propagation, the chromatic dispersion penalties favor narrower bandwidth AWGs. After 10-km SSMF the best trade-off between chromatic dispersion and RIN penalties is obtained for the 110-GHz AWG, being both the 55-GHz and the 220-GHz AWGs performances slightly under the enhanced 7%-overhead FEC limit [12].

Measurements have been repeated using digital electronic equalization, namely a 9-taps feed forward equalization (FFE) and a 4-taps decision feedback equalization (DFE). The received signal has been sampled by a 20-GSample digital storage oscilloscope and digital signal equalization has been performed with Matlab off-line post processing. Fig. 3 presents the obtained BER curves for 24-km SSMF transmission for the 110-GHz and 55-GHz AWG FWHMs. Both curves are below the enhanced FEC limit.

As shown in the previous measurements, chromatic dispersion plays a fundamental role in the transmission of the self-seeded signal. Investigation at 10 Gb/s has been thus initially focused on limitations at slightly different data rates, namely the 9.95328 Gb/s (corresponding to OC192) and the 10.7 Gb/s (corresponding to OTN G.709) rates. Then the performance of G.709 rate has been evaluated for various positive and negative dispersive loads. G.709 modulated optical spectra compared to CW optical spectra with two different 220-GHz and 110-GHz FWHM AWGs are shown respectively in Fig. 4a and in Fig. 4b, black traces refer to modulated spectra, while red traces are CW signals. Again it is evident that for larger AWG bandwidths the resulting output spectrum is wider. Fig. 4c and d present the respective back-to-back eye diagrams, recorded with a linear PIN photodiode. The associated extinction ratio (ER) is, in both cases, 5.5 dB, obtained with 110-mA RSOA bias current and 2.6-V peak-to-peak data voltage.

Fig. 5 presents the BER measurements obtained by an APD receiver followed by a commercially available clock and data recovery circuit with an electronic equalizer, namely a 9-taps FFE and a 4-taps DFE. The circle and triangle symbols refer respectively to OC192 and G.709 data rates. Black curves relate to the transmitter with 220-GHz FWHM AWG, while orange ones relate to the transmitter with 110-GHz FWHM AWG. The best performances are achieved with the slightly lower bit rate under all conditions: the limited

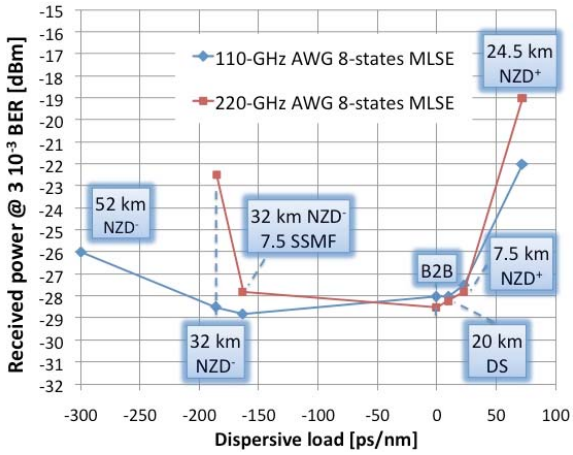

Fig. 6. Received power to achieve FEC limit for different dispersive loads, exploiting MLSE post processing at 10.7 Gb/s.

RSOA modulation bandwidth introduces a small amount of intersymbol interference. For comparison purposes, the back to back curve of an externally-modulated 300-kHz laser is plotted with open circles and dotted grey line for the OC192. The achieved ER is higher than 13 dB. For the transmitter with 220-GHz FWHM AWG, the back to back curves show an error floor well below the standard Reed-Solomon FEC limit ($1{\cdot}10^{-4}$ BER), negligible penalty is found after 20 km of propagation in a dispersion shifted (DS) fiber. For the transmitter with 110-GHz AWG, both back to back and 20-km DS fiber curves present an error floor well below enhanced 7%-overhead FEC limits. The penalty presented with respect to the externally modulated laser can be ascribed to the ER difference, which theoretically accounts for 2.8 dB, to the bandwidth limitation of the RSOA (E/O bandwidth 4 GHz) and to the higher RIN of the self-tuning source.

G.709 performance has been further analyzed for different positive and negative dispersion loads. The impact of chromatic dispersion has been tested exploiting different lengths of various dispersion fibers and two FWHM AWGs: 110 GHz and 220 GHz. In particular Fig. 6 presents the received power required to obtain a $3{\cdot}10^{-3}$ BER at 10.7 Gb/s, versus the accumulated dispersion; the received signal is sampled with the 20-G Sample digital storage oscilloscope and post processed to implement an 8-states maximum likelihood sequence estimation (MLSE) [13].

The transmitter with the 220-GHz AWG achieves a reach with a positive dispersion load up to 75 ps/nm and a negative dispersion load up to -185ps/nm. The transmitter with 110-GHz AWG allows on the other hand bridging up to 75-ps/nm positive dispersion load and up to -300-ps/nm negative dispersion load, which has been experimentally obtained with a 52-km long NZD$^-$ feeder fiber.

Fig. 6 asymmetric behavior as a function of the sign of the dispersive load enlightens that the main limitation to propagation is in this case determined by the chirp associated to the transmitter signal. This effect has been already experimentally found and discussed in [14] in relation with the negative chirp associated with RSOA direct modulation.

IV. Conclusion

We have experimentally demonstrated operation from 2.5 Gb/s up to 10.7 Gb/s of a network-embedded colorless self-tuning WDM transmitter for access applications, which exploits a remote FRM, located in proximity of the remote-node and shared among all the ONUs connected to the remote node, and a FR placed at the RSOA output. Arbitrary high-PDG RSOAs are allowed as the exploited retracing circuit guarantees that the polarization state at the RSOA input is always aligned to the RSOA high-gain transverse mode independently of the light journey into the retracing circuit, assuring a high round-trip gain and steady performance. The transmitter performances have been experimentally evaluated for 2.5 Gb/s and 5 Gb/s bit rates to evidence the chromatic dispersion penalty impact on transmission. For the 10 Gb/s rate, the performances have been analyzed both with positive and with negative dispersion loads: up to 52-km of NZD$^-$ fiber can be bridged, with an equivalent dispersive load of -300 ps/nm, exploiting a 110-GHz FWHM AWG and an 8-states MLSE equalization.

References

[1] S. H. Lee, *et al.*, "Athermal colourless C-band optical transmitter for passive optical networks," in *Proc. ECOC*, Torino, Italy, Sep. 2010, pp. 1–3, paper Mo1.B.2.

[2] S.-R. Moon, H.-K. Lee, and C.-H. Lee, "Automatic wavelength control method using rayleigh backscattering for WDM-PON with tunable lasers," in *Proc. CLEO 2011*, May, pp. 1–2, paper CFH1.

[3] N. Kashima, "Dynamic properties of FP-LD transmitters using side mode injection locking for LAN's and WDM-PONs," *J. Lightw. Technol.*, vol. 24, no. 8, pp. 3045–3058, Aug. 2006.

[4] S. J. Park, Y.-B. Choi, J.-M. Oh, S.-G. Koo, and D. Lee, "An evolution scenario of a broadband access network using R-SOA-based WDM-PON technologies," *J. Lightw. Technol.*, vol. 25, no. 11, pp. 3479–3487, Nov. 2007.

[5] Q. Deniel, *et al.*, "Up to 10 Gbit/s transmission in WDM-PON architecture using external cavity laser based on self-tuning ONU," in *Proc. OFC/NFOEC 2011*, Los Angeles, CA, USA, Mar., pp. 1–3, paper JTh2A.55.

[6] M. Presi and E. Ciaramella, "Stable self-seeding of reflective-SOAs for WDM-PONs," in *Proc. OFC/NFOEC 2011*, Los Angeles, CA, USA, Mar., pp. 1–3, paper OMP4.

[7] L. Marazzi, P. Parolari, R. Brenot, G. de Valicourt, and M. Martinelli, "Network-embedded self-tuning cavity for WDM-PON transmitter," *Opt. Express*, vol. 20, no. 4, pp. 3781–3786, 2012.

[8] M. P. C. M. Krijn, *et al.*, "Improved performance of compressively as well as tensile strained Quantum well lasers," *Appl. Phys. Lett.*, vol. 61, no. 15, pp. 1772–1774, Oct. 1992.

[9] M. Martinelli, L. Marazzi, P. Parolari, M. Brunero, and G. Gavioli, "Polarization in retracing circuits for WDM-PON," *IEEE Photon. Technol. Lett.*, vol. 24, no. 14, pp. 1191–1193, Jul. 15, 2012.

[10] M. Presi and E. Ciaramella, "Uncooled and polarization independent operation of self-seeded Fabry-Pérot Lasers for WDM-PONs," *IEEE Photon. Technol. Lett.*, vol. 24, no. 17, pp. 1523–1526, Sep. 1, 2012.

[11] A. D. McCoy, P. Horak, B. C. Thomsen, M. Ibsen, and D. J. Richardson, "Noise suppression of incoherent light using a gain-saturated SOA: Implications for spectrum-sliced WDM systems," *J. Lightw. Technol.*, vol. 23, no. 8, pp. 2399–2409, Aug. 2005.

[12] T. Mizuochi, "Next generation FEC for optical communication," in *Proc. OFC/NFOEC 2008*, San Diego, CA, USA, Feb., pp. 1–33, paper OTuE5.

[13] M. Rubsamen, J. M. Gené, P. J. Winzer, and R.-J. Essiambre, "ISI mitigation capability of MLSE direct-detection receivers," *IEEE Photon. Technol. Lett.*, vol. 20, no. 8, pp. 656–658, Apr. 15, 2008.

[14] K. Y. Cho, A. Agata, Y. Takushima, and Y. C. Chung, "Chromatic dispersion tolerance of 10-Gb/s WDM PON implemented by using bandwidth-limited RSOAs," in *Proc. OECC*, Jul. 2009, pp. 1–2, paper TuH2.